Journal of Sol-Gel Science and Technology (2019) 89:617–622
https://doi.org/10.1007/s10971-019-04923-6

BRIEF COMMUNICATION: SOL-GEL AND HYBRID MATERIALS WITH SURFACE MODIFICATION FOR APPLICATIONS

Synthesis of thiol-functionalized mesoporous silica nanoparticles for adsorption of Hg^{2+} from aqueous solution

Xinlong Yan[1] · Jinfeng Meng[1] · Xiaoyan Hu[1] · Rui Feng[1] · Min Zhou[1]

Received: 24 October 2018 / Accepted: 12 January 2019 / Published online: 28 January 2019

Abstract

Development of new adsorbents for efficient capturing of mercury (Hg(II)) ions from aqueous solution is of significant importance in environmental area. In this work, mesoporous silica nanoparticles with different morphologies (flower-like nanospheres with wrinkles, nanoparticles with concavities and sunken nanovesicles) were prepared and functionalized with 3-mercaptopropyltrimethoxysilane (MPTS). The as-prepared materials were characterized by different technics and applied for Hg^{2+} removal from aqueous solution. The sample with flower-like nanospheres morphology exhibited highest surface area and pore volume among the three silica samples, and the corresponding S-H groups functionalized nanospheres showed the highest adsorption capacity of 479 mg/g and fast adsorption rate for Hg^{2+}. The isotherm and kinetics data fitted well with the Langmuir isotherm and the pseudo-second-order kinetics model, respectively. Furthermore, the above adsorbent could be easily regenerated and the regeneration efficiency could remain 94% up to three cycles of the regeneration.

Graphical Abstract

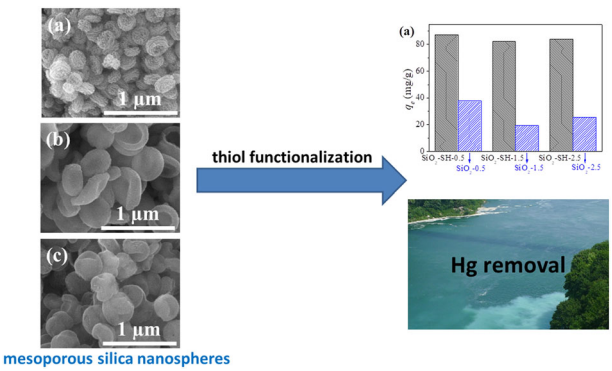

Supplementary information The online version of this article (https://doi.org/10.1007/s10971-019-04923-6) contains supplementary material, which is available to authorized users.

✉ Xinlong Yan
yanxl@cumt.edu.cn

[1] Key Laboratory of Coal Processing and Efficient Utilization (Ministry of Education), School of Chemical Engineering & Technology, China University of Mining and Technology, 221116 XuZhou, China

Highlights

- Thiol-functionalized silica nanoparticles with different morphology were prepared.
- The functionalized nanoparticles exhibited high Hg^{2+} adsorption capacity of 479 mg/g.
- The thiol-functionalized silica can adsorb Hg^{2+} quickly and be regenerated easily.

Keywords Thiol functionalization · Mesoporous silica · Mercury · Adsorption

1 Introduction

With the rapid development of industry, water pollution caused by releasing of heavy metals has become a serious environmental problem. As a typical hypertoxic heavy metal, mercury (Hg(II)) is usually released directly to the environment through dissolving in liquids, and effectively removing aqueous Hg(II) has been a major challenge [1–3]. Various technologies have been developed to remove Hg from water, such as chemical precipitation, adsorption, and ion exchange etc [4–6]. Among these techniques, adsorptive removal is considered to be the most effective and economic one [7–9]. To date, a wide variety of adsorbents have been studied for Hg removal, however, conventional adsorbents often have several disadvantages such as low adsorption capacity and selectivity [10–12].

It has been recognized that incorporation of thiol groups onto porous materials could enhance the capture of heavy metals from aqueous solution, and the support materials often played a vital role [13, 14]. Although different porous supports such as SBA-15 [15], vermiculite [16], and Coal Fly Ash [17] have been investigated for the Hg^{2+} adsorption, these adsorbents suffer from some drawbacks such as low grafted amount of thiols and poor recyclability. Thus, development of new support materials is still urgent.

In this work, mesoporous silica nanoparticles with different morphologies were prepared and used as support materials for incorporation of thiol groups. In addition, factors affecting adsorption of Hg by the above materials were investigated, including adsorption kinetics, adsorption isotherms, and recyclability.

2 Experimental

2.1 Synthesis of mesoporous silica nanoparticles

The mesoporous silica nanoparticles were synthesized according to a reported method with minor changes [18]. In a typical procedure, 1.750 g of cetyltrimethylammonium bromide was dissolved into a mixture of 100 mL of deionized water and 25 mL of ethanol. Then, 2.5 mL of 1-Pentanol was added to the above solution. After stirring for 5 min, different amount of $NH_3{\cdot}H_2O$ (0.5, 1.5, or 2.5 mL) and 11 mL of tetraethoxysilane were added, resulting in the formation of white precipitate, followed by continuous stirring for 6 h at 40 °C. Subsequently, the precipitate was separated and washed with deionized water and ethanol for several times, and then dried at 50 °C in air. Finally, the as-prepared silica was calcined at 600 °C for 2 h in air. The obtained samples were labeled as SiO_2-x, where x represents the amount of $NH_3{\cdot}H_2O$ added during the synthesis.

2.2 Synthesis of thiol-functionalized mesoporous silica nanoparticles

Thiol-functionalized mesoporous silica nanoparticles were prepared by the following procedure. First, 5 mL of 3-mercaptopropyltrimethoxysilane (MPTS) was dropped into a suspension containing 50 mg of the as-prepared SiO_2 nanoparticles dispersed in 30 mL of dried toluene. Then, the mixture was refluxed at 90 °C for 12 h. Finally, the white product was collected by centrifugation, washed several times with toluene and methanol, and dried at 80 °C for 12 h. The prepared sample was marked as SiO_2-SH.

2.3 Characterization

The morphology of the samples was taken with a FEI Quanta 400 FEG scanning electron microscope (SEM). N_2 adsorption–desorption isotherms were measured in a Quantachrome iQ2 porosimeter after sample degassing at 100 °C overnight. The pore size distribution was analyzed using Barrett–Joyner–Halenda (BJH) method based on the desorption branch. Average pore diameter was calculated as 4 V/A (V: pore volume; A: surface area). Thermogravimetric analysis (TGA, Netzsch STA 449 F5) measurement was performed under Ar gas at a flow rate of 100 cm^3/min and a temperature ramp rate of 10 °C/min. Fourier-Transform Infrared (FT-IR) spectra were measured with a Thermo Nicolet iS5 spectrometer.

2.4 Adsorption

Typically, 10 mg of adsorbent was put into 100 mL of Hg^{2+} solution with different concentrations. The mixture was drawn at regular intervals and filtered by a 0.45 μm filter membrane for analysis. The concentration of Hg^{2+} was measured with an elemental mercury analyzer (DMA-80).

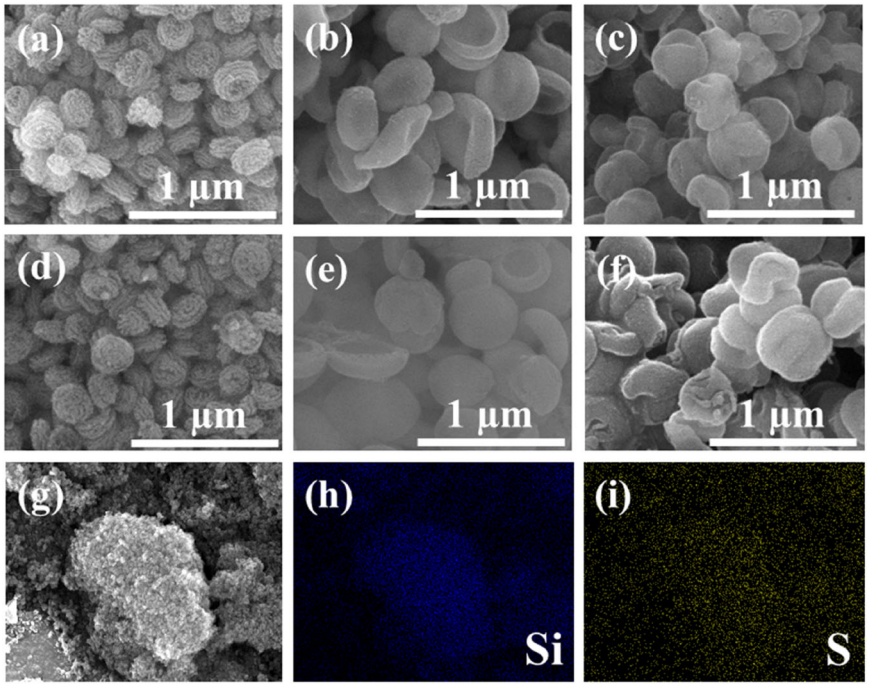

Fig. 1 Scanning electron microscope (SEM) images of **a** SiO_2-0.5, **b** SiO_2-1.5, **c** SiO_2-2.5, **d** SiO_2-SH-0.5, **e** SiO_2-SH-1.5, **f** SiO_2-SH-2.5, and **g** elemental mappings (×7378 magnification) of **h** Si and **i** S of SiO_2-SH-0.5

3 Results and discussion

The morphologies of silica nanoparticles prepared with different amount of $NH_3{\cdot}H_2O$ are shown in Figs. 1a−c. It can be clearly seen that the sample prepared with 0.5 mL of $NH_3{\cdot}H_2O$ shows a flower-like nanospheres with wrinkles on its surface and has an average diameter of about 280 nm. With the amount of ammonia increased to 1.5 mL, the surface of nanoparticles became smooth with appearance of some concavities. There is also an increase of the diameter to around 400 nm. Further increasing the ammonia amount to 2.5 mL, sunken nanovesicles can be observed with diameter of 360 nm. The morphologies of nanoparticles prepared here are consistent with the reported results [18]. However, the particle size became larger, especially for sample SiO_2-0.5 and SiO_2-1.5, which may be due to the relatively large-scale preparation. With surface modification with MPTS, the morphologies of those silica nanoparticles show little change, as revealed in Figs. 1d−f. The MPTS on the surface of silica was investigated by Energy dispersive X-ray (EDX) elemental mapping, as shown in Figs. 1g−i, S element from MPTS could be detected and uniformly dispersed on the surface of silica nanoparticles, which suggests successful incorporation of mercaptopropyl group on the silica.

The functional groups on the silica and MPTS modified silica was investigated by FT-IR (Fig. 2a). A broad peak at 3439 cm^{-1} and a strong peak around 1091 cm^{-1} are observed for all samples, which can be assigned to silanol -OH stretching and asymmetric Si-O-Si vibrations, respectively [19]. After modification with MPTS, a very weak peak appeared at 2560 cm^{-1} can be assigned to the -SH group [20], which further confirmed the successful grafting of S-H groups onto the silica. The surface area and porosity data of the materials are summarized in Table 1 and N_2 adsorption–desorption isotherms of SiO_2 and modified SiO_2 are depicted in Fig. 2b and Fig. S1. It could be seen that SiO2-0.5 shows type IV isotherm with an obvious hysteresis loop at high relative pressure. The SiO_2-0.5 shows the highest surface area and pore volume. There is a small decrease of surface area and pore volume with increasing ammonia amount for the SiO_2 samples. However, a significant reduction of them is observed for MPTS modified SiO_2, which should be attributed to occupation of the pores by organic groups. Interestingly, greater extent of loss in surface area was obtained for SiO_2-1.5 and SiO_2-2.5 ($> 66\%$) after surface functionalization, compared with that of SiO_2-0.5 (with a loss of ~52). This phenomenon should be associated with relatively small pore size of the former, as partial pores in them may impede the entry of the organic groups during the functionalization.

The TGA analysis of pure SiO_2 and surface modified SiO_2 samples were shown in Fig. S2. For pure SiO_2 samples, an initial weight loss at < 100 °C was due to loss of adsorbed water molecule and little weight change can be seen with further increasing temperature. Whereas, for SiO_2-SH samples, weight loss at temperature lower than 100 °C was smaller, and this was due to the presence of the hydrophobic mercaptopropyl group on the surface of silica [20]. Moreover, a weight loss at temperature > 300 °C could be assigned to the decomposition of mercaptopropyl group. The calculated mass loss between 300 and 800 °C was 17, 10, and 12% for SiO_2-SH-0.5, SiO_2-SH-1.5, and SiO_2-SH-2.5,

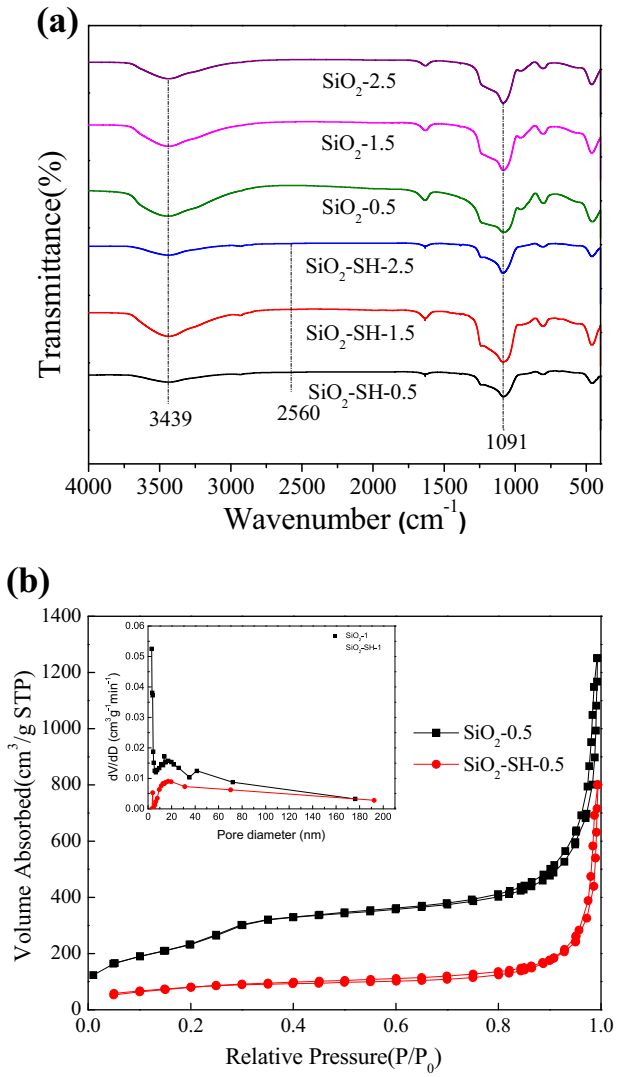

Fig. 2 **a** FT-IR of different SiO_2 and SiO_2-SH samples and **b** N_2 adsorption-desorption isotherms of SiO_2 -0.5 and SiO_2-SH-0.5 (the insert is the corresponding pore size distributions)

Table 1 The surface area and pore properties of SiO_2 and SiO_2-SH samples

Samples	BET surface area (m^2/g)	Pore volume (cm^3/g)	Average pore size (nm)
SiO_2-0.5	1046.3	1.9	9.0
SiO_2-1.5	869.0	1.0	3.7
SiO_2-2.5	904.6	0.8	3.6
SiO_2-SH-0.5	499.5	1.2	16.2
SiO_2-SH-1.5	295.6	0.7	5.5
SiO_2-SH-2.5	305.9	0.5	6.6

respectively, indicating that SiO_2-SH-0.5 owns the most mercaptopropyl groups on its surface.

The adsorption capacities of different SiO_2 and SiO_2-SH for Hg^{2+} was comparatively studied (initial $C_{Hg(II)} = 100$ mg/L, T = 30 °C) and the results are shown in Fig. 3a. Pure SiO_2 adsorbed small amount of Hg^{2+}, after modification, the adsorption capacity improved dramatically. Among all the samples, SiO_2-SH-0.5 exhibited the highest adsorption capacity of 87.3 mg/g, in virtue of the highest amount of mercaptopropyl group and surface area. Consequently,

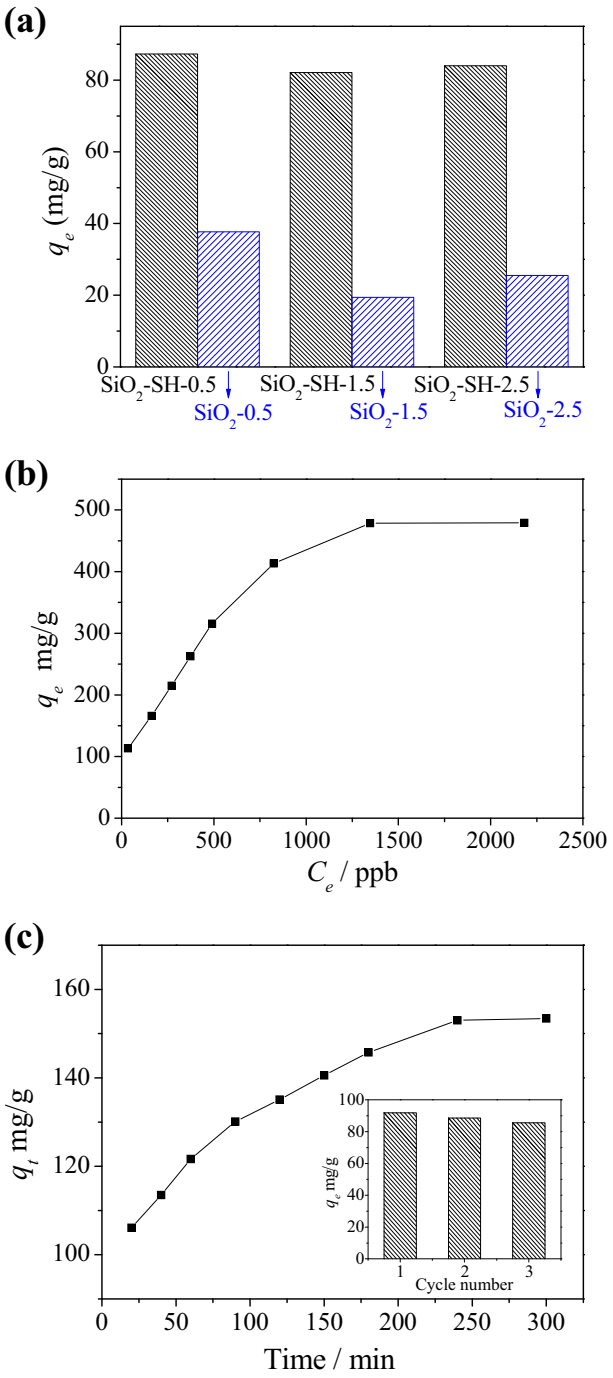

Fig. 3 **a** Adsorption capacity of different SiO_2 and SiO_2-SH samples for Hg^{2+}, **b** adsorption isotherm of Hg^{2+} on SiO_2-SH-0.5, and **c** effect of contact time on adsorption of Hg^{2+} on SiO_2-SH-0.5 (the insert is the recyclability of SiO_2-SH-0.5)

SiO_2-SH-0.5 was selected for further study. The effects of initial Hg^{2+} concentration and contact time on the adsorption are shown in Figs. 3b, c, respectively. There is a rapid increase of adsorption capacity at initial stage and gradual stabilization as the initial Hg^{2+} concentration increased. The saturated adsorption capacity could be as high as 479 mg/g, which was much higher than other recently reported SH-functionalized sorbents, such as thiol modified Fe_3O_4@-SiO_2@C (184 mg/g) [21], Fe_3O_4@$Cu_3(btc)_2$ (348.43 mg/g) [22] and mercaptoamine-functionalized silica-coated magnetic nanoparticles (355 mg/g) [23]. It is also comparable with those of thiopyrene-containing porous carbon (518 mg/g) [24], MoS_4^{2-} intercalated Layered double hydroxides (LDH) (500 mg/g) [25] and MOF (Metal-organic frameworks) FJI-H12 (439.8 mg/g) [26]. Figure 3c reveals that the adsorption process can be completed in 4 h, which demonstrated a rapid adsorption of Hg^{2+} with SiO_2-SH-0.5.

Different typical isotherm and kinetic models have been used to further describe the adsorption behavior of SiO_2-SH-0.5 for Hg removal. And their equations are shown in supporting information. Fig. S3 showed the fitting results of Langmuir and Freundlich isotherm models, and the parameters are presented in Table S1. It is found that Langmuir model provided a better fit to the adsorption data than Freundlich model, with higher correlation coefficient ($R^2 >$ 0.976). Moreover, the maximum adsorption capacity calculated by Langmuir equation was closer to the value obtained by experiment. This suggests that a monolayer adsorption occurred on the surface of SiO_2-SH-0.5. The kinetic data are formulated by the pseudo-first-order model and pseudo-second-order model, respectively (Fig. S4). Compared with the pseudo-first-order model, the pseudo-second-order model gives better correlation coefficient (> 0.998) for Hg^{2+} adsorption, and the calculated adsorption capacity is in good agreement with the experiment value (Table S2). This result indicates that the adsorption of Hg^{2+} by SiO_2-SH-0.5 follows the pseudo-second-order model, and chemisorption may be involved in the adsorption process [27, 28].

After adsorption, SiO_2-SH-0.5 was regenerated by washing with HCl solution (1 M) containing 1 wt. % of thiourea and subsequent separation and drying in air. Then, the recyclability was evaluated, and the results show that SiO_2-SH-0.5 exhibit good reuse stability, for >94% of its original capacity could be retained after three adsorption–desorption cycles (Fig. 3c).

4 Conclusions

Three mesoporous silica nanoparticles with different morphologies were prepared by adjusting amount of ammonia during the synthesis. The sample with flower-like nanospheres morphology exhibited highest surface area and pore volume. Then the as-prepared silica nanoparticles were functionalized with MPTS and used as adsorbent for Hg^{2+} removal from aqueous solution. After modification, the sample with flower-like nanospheres morphology shows a highest Hg^{2+} adsorption capacity of 479 mg/g. Besides, the above adsorbent can adsorb Hg^{2+} quickly and be easily regenerated, which makes it potential to be an effective and promising adsorbent for Hg^{2+} removal.

Acknowledgements This work was supported by the Fundamental Research Funds for the Central Universities (no. 2018XKQYMS18) and the Priority Academic Program Development of Jiangsu Higher Education Institutions.

Compliance with ethical standards

Conflict of interest The authors declare that they have no conflict of interest.

Publisher's note: Springer Nature remains neutral with regard to jurisdictional claims in published maps and institutional affiliations.

References

1. Abbas A, Al-Amer AM, Laoui T et al. (2016) Heavy metal removal from aqueous solution by advanced carbon nanotubes: critical review of adsorption applications. Sep Purif Technol 157:141–161
2. Xiong CH, Li YL, Wang GT, Fang L, Zhou SG, Yao CP, Chen Q, Zheng XM, Qi DM, Fu YQ, Zhu YF (2015) Selective removal of Hg(II) with polyacrylonitrile-2-amino-1,3,4-thiadiazole chelating resin: batch and column study. Chem Eng J 259:257–265
3. Ma YX, Xing D, Shao WJ, Du XY, La PQ (2017) Preparation of polyamidoamine dendrimers functionalized magnetic graphene oxide for the adsorption of Hg(II) in aqueous solution. J Colloid Interface Sci 505:352–363
4. Oehmen A, Vergel D, Fradinho J, Reis MA et al. (2014) Mercury removal from water streams through the ion exchange membrane bioreactor concept. J Hazard Mater 264:65–70
5. Mohan D, Sarswat A, Ok YS et al. (2014) Organic and inorganic contaminants removal from water with biochar, a renewable, low cost and sustainable adsorbent–a critical review. Bioresour Technol 160:191–202
6. Soylak M, Erdogan ND (2006) Copper (II) rubeanic acid coprecipitation system for separation-preconcentration of trace metal ions in environmental samples for their flame atomic absorption spectrometric determinations. J Hazard Mater 137:1035–1041
7. Bo X, Dong L, Han L, Gu H (2017) 3D hierarchical flower-like nickel ferrite/manganese dioxide toward lead (II) removal from aqueous water. J Hazard Mater 325:178–188
8. Viltužnik B, Košak A, Zub YL et al. (2013) Removal of Pb(II) ions from aqueous systems using thiol-functionalized cobalt-ferrite magnetic nanoparticles. J Sol-Gel Sci Technol 68:365–373
9. Zhang J, Yan X, Hu X, Feng R, Zhou M (2018) Direct carbonization of Zn/Co zeolitic iimidazolate frameworks for efficient adsorption of rhodamine B. Chem Eng J 347:640–647
10. Blanchard G, Maunaye M, Martin G (1984) Removal of heavy metals from waters by means of natural zeolites. Water Res 18:1501–1507

11. Benhammou A, Yaacoubi A, Nibou L, Tanouti B (2005) Adsorption of metal ions onto Moroccan stevensite: kinetic and isotherm studies. J Colloid Interface Sci 282:320–326
12. Meríbofí L, Royuela S, Zamora F et al. (2017) Thiol grafted imine-based covalent organic frameworks for water remediation through selective removal of Hg(II). J Mater Chem A 34:17973–17981
13. Melnyk IV, Pogorilyi RP, Zub YL et al. (2018) Protection of thiol groups on the surface of magnetic adsorbents and their application for wastewater treatment. Sci Rep 8:8592
14. Melnyk IV, Nazarchuk GI, Václavíková M, Zub YL (2018) IR spectroscopy study of SBA-15 silicas functionalized with the ethylthiocarbamidepropyl groups and their interactions with Ag (I) and Hg (II) ions. Appl Nanosci (2018). https://doi.org/10.1007/s13204-018-0761-5
15. Mureseanu M, Reiss A, Stefanescu I et al. (2008) Modified SBA-15 mesoporous silica for heavy metal ions remediation. Chemosphere 73:1499–1504
16. Nascimento FHD, Costa DMDS, Masini JC (2016) Evaluation of thiol-modified vermiculite for removal of Hg(II) from aqueous solutions. Appl Clay Sci S124 125:227–235
17. Hakami O, Zhang Y, Banks CJ (2012) Thiol-functionalised mesoporous silica-coated magnetite nanoparticles for high efficiency removal and recovery of Hg from water. Water Res 46:3913–3922
18. Chen J, Sheng Y, Song Y et al. (2018) Multimorphology mesoporous silica nanoparticles for dye adsorption and multicolor luminescence applications. ACS sustain. Chem Eng 6:3533–3545
19. Sheng J, Xu Y, Yu J, Ding B (2017) Robust fluorine-free superhydrophobic amino-silicone Oil/SiO_2 modification of electrospun polyacrylonitrile membranes for waterproof-breathable application. ACS Appl Mater Interfaces 9:15139–15147
20. Dash S, Chaudhuri H, Gupta R et al. (2017) Fabrication and application of low-cost thiol functionalized coal fly ash for selective adsorption of heavy toxic metal ions from water. Ind Eng Chem Res 56:1461–1470
21. Shi Z, Xu C, Lu P et al. (2018) Preparation and the adsorption ability of thiolated magnetic core-shell Fe_3O_4@SiO_2@C-sh for removing Hg^{2+}, in water solution. Mater Lett 225:130–133
22. Ke F, Jiang J, Li Y et al. (2017) Highly selective removal of Hg^{2+} and Pb^{2+} by thiol-functionalized Fe_3O_4@metal-organic framework core-shell magnetic microspheres. Appl Surf Sci 413:266–274
23. Bao S, Li K, Ning P et al. (2017) Highly effective removal of mercury and lead ions from wastewater by mercaptoamine-functionalised silica-coated magnetic nano-adsorbents: behaviours and mechanisms. Appl Surf Sci 393:457–466
24. Shin Y, Fryxell GE, Um W, Parker K, Mattigod SV, Skaggs R (2007) Sulfur-functionalized mesoporous carbon. Adv Funct Mater 17:2897–2901
25. Ma L, Wang Q, Islam SM, Liu Y, Ma S, Kanatzidis MG (2016) Highly selective and efficient removal of heavy metals by layered double hydroxide intercalated with the MoS_4^{2-} ion. J Am Chem Soc 138:2858–2866
26. Liang L, Chen Q, Jiang F, Yuan D, Qian J, Lv G, Xue H, Liu L, Jiang H-L, Hong M (2016) In situ large-scale construction of sulfur-functionalized metal-organic framework and its efficient removal of Hg(II) from water. J Mater Chem A 4:15370–15374
27. Jiang N, Xu Y, Dai Y, Luo W, Dai L (2012) Polyaniline nanofibers assembled onalginate microsphere for Cu^{2+} and Pb^{2+} uptake. J Hazard Mater 215- 216:17–24
28. Zhang J, Yan X, Hu M, Hu X, Zhou M (2018) Adsorption of Congo red from aqueous solution using ZnO modified SiO_2 nanospheres with rough surfaces. J Mol Liq 249:772–778